Available online at www.sciencedirect.com
SCIENCE DIRECT
Energy and Buildings 38 (2006) 743–757
ENERGY and BUILDINGS
www.elsevier.com/locate/enbuild

Evaluation methods and development of a new glare prediction model for daylight environments with the use of CCD cameras

Jan Wienold [a,*], Jens Christoffersen [b]

[a] *Fraunhofer Institute for Solar Energy Systems, Heidenhofstr. 2, 79110 Freiburg, Germany*
[b] *Danish Building Research Institute, Dr. Neergaards vej 15, 2970 Hoersholm, Denmark*

Abstract

Daylighting and the impact of daylighting strategies on the visual environment continue to be a vital issue for building occupants due to visual comfort and user acceptance of luminous indoor environments. Some of the critical factors affecting the level of visual comfort and quality in daylit office spaces include glare, window luminances, and luminance ratios within the field of view. One of the goals of this study was to provide new insight into the impact of luminance distributions on glare. The luminance distribution within the field of view was recorded using CCD camera-based luminance mapping technology. The technology provides a great potential for improved understandings of the relation between measured lighting conditions and user response. With the development of the RADIANCE based evaluation tool ''evalglare'', it became possible to analyse glare according to a number of daylight glare prediction models as well as contrast ratios in various daylit situations (workplace, VDU). User assessments at two locations (Copenhagen, Freiburg) with more than 70 subjects under various daylighting conditions were performed in order to assess existing glare models and to provide a reliable database for the development of a new glare prediction model. The comparison of the results of the user assessments with existing models clearly shows the great potential for improving glare prediction models. For the window luminance a squared correlation factor of only 0.12 and for the daylight glare index (DGI) of 0.56 were found. Due to the low predictive power of existing glare prediction models a new index, *daylight glare probability (DGP)*, was developed and is presented in this paper. DGP is a function of the vertical eye illuminance as well as on the glare source luminance, its solid angle and its position index. The DGP showed a very strong correlation (squared correlation factor of 0.94) with the user's response regarding glare perception.

Keywords: Daylight; Comfort; Discomfort glare; RADIANCE; CCD camera; Daylight glare probability

1. Introduction

In a world concerned with climate change and global warming, daylighting buildings as part of an overall sustainable design strategy is often presented as being part of the 'solution'. Daylighting has been shown to provide many benefits to building occupants ranging from improved health and well-being to increased lighting quality [1]. However, daylight design requires careful system integration. Daylight varies in intensity, colour and direction over time. These variations are one of the design parameters which are difficult to cope with since they have a great impact on both the thermal and the visual environment.

Ongoing developments of new glazing technologies and shading devices result in an increasing selection of new façade solutions. This is reflected in recent European architecture as glass is increasingly being used in buildings.

Successful daylighting requires trade-offs and optimisation between competing design aspects such as façade layout, space configuration, and the choice of lighting system used. The task at hand is to identify the most appropriate optical glazing properties that provide adequate daylight levels while avoiding glare and excessive heat gains. This process requires reliable tools and/or descriptors for different aspects of comfort and energy demand. For many aspects reliable tools are available – but not for discomfort glare from windows (neither tools nor descriptors).

The objective of this study was to investigate the user perception of solar shading systems regarding glare by using laboratory tests with subjects, to compare the results with

* Corresponding author. Tel.: +49 761 4588 5133; fax: +49 761 4588 9133.
E-mail address: jan.wienold@ise.fraunhofer.de (J. Wienold).

0378-7788/$ – see front matter © 2006 Elsevier B.V. All rights reserved.
doi:10.1016/j.enbuild.2006.03.017

Nomenclature

$A_{façade}$	Façade area (m^2)
A_{glas}	Glazed area (m^2)
CGI	CIE glare index
D	distance eye – to plane of source in view direction
DGI	daylight glare index
DGP	daylight glare probability
E_d	direct vertical illuminance at eye due to all sources (lux)
E_i	indirect vertical illuminance at eye (lux)
E_v	vertical illuminance at eye-level (lux)
H	vertical distance between source and view direction
L_b	background luminance (cd/m^2)
L_s	glare source luminance (cd/m^2)
P	Guth's position index
u-value	heat loss coefficient (W/m^2 K)
Y	horizontal distance between source and view direction

Greek letters

$\rho_{ceiling}$	total reflectance of ceiling in visible spectrum
ρ_{floor}	total reflectance of floor in visible spectrum
ρ_{vis}	total reflectance in visible spectrum
ρ_{wall}	total reflectance of wall in visible spectrum
σ	angle between line of sight and line from observer to source (°)
τ	angle from vertical of plane containing source and line of sight (°)
$\tau_\perp$	total transmission of glazing in visible spectrum for perpendicular angle of incidence
ω_s	solid angle subtended by the source (sr)
Ψ	angular displacement of the glare source from the observer's line of sight
Ω_s	solid angle subtended by the source, modified by the position of the source (sr)

existing glare rating equations, and to derive a new glare prediction model. In the tests typical office tasks and viewing directions were investigated in order to derive a reliable glare rating. The laboratory tests were conducted at the Danish Building Research Institute (SBi, Denmark) and at the Fraunhofer Institute for Solar Energy Systems (ISE, Germany).

2. Discomfort glare

The aim of a good daylight design is first, to provide fully sufficient light for efficient visual performance, and second, to ensure a comfortable and pleasing environment appropriate to its purpose. The comfort aspect of a daylight design is closely related to the problem of glare [3]. Estimating the magnitude of glare is only possible by characterisations and assessments made by the subject involved, together with the physical factors (e.g. source luminance, solid angle of the glare source, background luminance, etc.). A number of previous experimental studies on subjective glare sensation resulted in glare indices that describe the subjective magnitude of glare discomfort with high values illustrating, e.g. uncomfortable or intolerable sensation of discomfort. Several different equations describing the subjective sensation of discomfort glare experienced by an observer have been published. All of these equations were derived from experiments with artificial glare sources – none of them under real daylight conditions. In general, all these equations draw upon the four physical quantities shown in Eq. (1) [4]

$$G = \left(\frac{L_s^e \omega_s^f}{L_b^g f(\Psi)} \right) \tag{1}$$

The glare constant G expresses the subjective sensation and e, f and g are weighting exponents, while $f(\Psi)$ is a complex function of the displacement angle. The other parameters are

- The luminance (L_s) of the glare source. In the case of windows: the luminance of the sky as seen through the window (the brighter the source or sky, the higher the index);
- The solid angle subtended by the source (ω_s). In the case of windows: the apparent size of the visible area of sky at the observer's eyes (the larger the area, the higher the index);
- The angular displacement (Ψ) of the source from the observer's line of sight. In the case of windows: the position of the visible sky within the field of view (the further from the centre of vision, the lower the index);
- The general field of luminance (L_b) controlling the adaptation levels of the observer's eye (also called the background luminance). In the case of windows: the average luminances of the room excluding the visible sky (the brighter the room, the lower the index).

Some of the more commonly referred to indices are listed and briefly discussed below, namely

- BRS glare equation (BRS or BGI);
- Cornell equation or daylight glare index (DGI);
- CIE Glare Index (CGI);
- Unified Glare Rating (UGR);

2.1. BRS glare equation (BRS or BGI)

In 1950 Petherbridge and Hopkinson [5] developed the BRS glare equation at the Building Research Station in England. The sensation of glare was rated in accordance with the following degrees of sensation: just noticeable, just acceptable, just uncomfortable and just intolerable. The empirically developed equation has the form

$$\mathrm{BGI} = 10 \log_{10} 0.478 \sum_{i=1}^{n} \frac{L_s^{1.6} \omega_s^{0.8}}{L_b P^{1.6}} \tag{2}$$

where

- Guth's position index P, expresses the change in discomfort glare experienced relative to the azimuth and elevation of the source and position the observer's line of sight;
- n number of glare sources.

The BGI is limited to small sources with solid angles inferior to 0.027 sr [7]. Chauvel et al. [9] stated that BGI does not predict glare from larger sources accurately and does not take into account the effect of adaptation. Iwata et al. [10] compared BGI with DGI and CGI (see below) and demonstrated that BGI was the least accurate when using a wide light source. They stated that BGI had originally been intended for a small point source and not a large wide source.

2.2. Cornell equation or daylight glare index (DGI)

The Cornell glare equation is a modification of the British glare index, and adapted to predict glare from a large source (window). The study was conducted at the BRE and Cornell University (USA) ([6,9]). The equation was developed through experiments using fluorescent lamps behind an opal-diffusing screen. The equation is expressed as follows:

$$\mathrm{GI} = 10\log_{10} 0.48\sum_{i=1}^{n}\frac{L_\mathrm{s}^{1.6}\Omega_s^{0.8}}{L_\mathrm{b}+0.07\,\omega_\mathrm{s}^{0.5}L_\mathrm{s}} \tag{3}$$

where Ω_s (sr) is the solid angle subtended by the glare source modified by the position of the source with respect to field of view and Guth's position index.

Validation studies of this equation show that the correlation between glare from windows and predicted glare is not as strong as in the case of artificial lighting. There is a greater tolerance of mild degrees of glare from windows than from a comparable artificial lighting situation, but the tolerance does not extend to severe degrees of glare [11,9].

2.3. CIE glare index (CGI)

The CIE adopted the following equation proposed by Einhorn [12,13] as a unified glare assessment method

$$\mathrm{CGI} = 8\log_{10} 2\frac{[1+(E_\mathrm{d}/500)]}{E_\mathrm{d}+E_i}\sum_{i=1}^{n}\frac{L_\mathrm{s}^2\omega_\mathrm{s}}{P^2} \tag{4}$$

where

- Ed (lx) is the direct vertical illuminance at the eye due to all sources;
- Ei (lx) is the indirect illuminance at the eye (Ei = πL_b).

The CGI was developed in order to correct the mathematical inconsistency of the BRS equation for multiple glare sources.

2.4. CIE's unified glare rating system (UGR)

The CIE [14] proposed a unified glare rating system (UGR), which incorporates Guth's position index and combines aspects of CGI and BGI to evaluate glare sensations for an artificial lighting system (restricted to sources with a solid angle of 3×10^{-4} to 10^{-1} sr). The equation is

$$\mathrm{UGR} = 8\log_{10}\frac{0.25}{L_\mathrm{b}}\sum_{i=1}^{n}\frac{L_\mathrm{s}^2\,\omega_\mathrm{s}}{P^2} \tag{5}$$

3. Method of the user assesments

3.1. Test facilities

User assessments were conducted at the Danish Building Research Institute (SBi, Denmark) and at Fraunhofer Institute for Solar Energy Systems (ISE, Germany). Both institutions carried out the experiment using the same procedure and under almost identical experimental conditions [2]. The study was performed at each location in two identical experimental rooms, one with subjects (test room), and the other with measuring equipment (reference room). Each room was equipped with one workstation (a desk, an office chair, and a computer). The work place was next to the window and subjects were seated 1.5 m away from the window. Only flat panel displays (Eizo FlexScan L565, max. self-luminance 190 cd/m^2) were used.

The Danish daylight laboratory is located in Hoersholm, north of Copenhagen (latitude 55.86°N, longitude 12.49°E). The laboratory has two south-oriented experimental rooms, which can be changed so that north and east orientations can also be studied. The rooms are orientated 7° east of due south to allow maximum amounts of sunlight to fall on to the glazing, but with some outside obstructions to the west. The two rooms are characterised by identical photometrical ($\rho_\mathrm{wall}=0.62$, $\rho_\mathrm{ceiling}=0.88$, $\rho_\mathrm{floor}=0.11$) and geometrical features (3.5 m wide, 6.0 m deep, 3.0 m high). The rooms have a glass area covering the whole façade and the glazing was Low-E double-glass with a light transmission of $\tau_\perp=72\%$, u-value of 1.1 W/m^2 °C and a total solar energy transmission of 59%.

The German daylight laboratory is located in the south-western part of Germany in Freiburg (latitude 48.01°N, longitude 7.84°E). The experimental rooms are sited on the roof of the Fraunhofer ISE office building and they can be fully rotated without restrictions, which allows a wide range of sun altitude and azimuth to be studied, quite independent of the season. The two rooms have identical photometrical ($r_\mathrm{wall}=0.56$, $r_\mathrm{ceiling}=0.80$, $r_\mathrm{floor}=0.34$) and geometrical features (3.65 m wide, 4.6 m deep, 3.0 m high). The distance from floor to the suspended ceiling can be changed. The rooms have a glass area covering the whole façade and the glazing is colour-neutral sun protective double-glass with a light transmission of $\tau_\perp=54\%$, a u-value of 1.1 W/m^2 °C, and a total solar energy transmission of 29%.

Fig. 1. Photographs of the Fraunhofer ISE test facility with the three window configurations (left: small window, middle: medium window, right: large window). The rooms can be rotated fully in order to be more or less independent on seasons to set up a defined angle of incidence for the sun.

In this study, subjects were exposed, at both locations, to three different window arrangements typical for today's design of windows in office buildings. The window arrangements could be changed within 5 min, as the fully glazed façade could be either partially occluded (small and medium sized windows) or totally exposed (large window). These three different window sizes included a small window in the centre of the façade (sill-height at workplane), a medium rectangular window covering the width of the façade (same window-height as the small window) and a large window covering the whole façade (see Fig. 1).

The glazed areas at both locations and the corresponding solid angles of the source are shown in Table 1

Three different solar shading devices were included in the study in order to have variations in potential glare situations. All Venetian blind systems were operated using customized stepper motors connected to a LON bus to ensure the same tilt angle of the slats in both rooms (Tables 2 and 3).

3.2. Interior and exterior measurements

The indoor illuminance on the work plane in the reference room was monitored with five sensors (Hagner Model SD2) at regular distances fixed on metal supports 0.85 m from the floor. To verify that both rooms had the same illuminance level during the tests, two sensors in both rooms were installed at the same position; a horizontal illuminance sensor near the subject and a vertical sensor at a VDT screen facing the subject. A vertical illuminance sensor was mounted on a tripod at a height of 1.2 m to measure the vertical illuminance (reference room) at the approximate position of the subject's eyes (see Fig. 2).

The illuminance measurements were made every 10 s at ISE. At SBi illuminance measurements were made every 30 s.

The luminance distribution within the field of view of the subjects was measured using a calibrated, scientific-grade CCD camera from TechnoTeam (ISE: LMK 98-2 Luminance VideoPhotometer, SBi: LMK Mobile, both with a Nikon FC-E8 lens, field of view (FOV) 183°). The CCD camera was mounted on a tripod together with the vertical illuminance sensor measuring the eye illuminance level. The resulting digital image from LMK98-2 contained 1300 (horizontal) by 1030 (vertical) pixels corresponding to as many luminance values. The LMK Mobile contained 1280 (horizontal) by 1024 (vertical) pixels. Both had a V(λ) correction and the LMK98-2 had a dynamic range varying from less than 3 cd/m^2 to approximately 1.8×10^6 cd/m^2, while the range of the LMK Mobile was 3–200,000 cd/m^2. The cameras came equipped with software that allowed control of the camera

Table 1
Glazed area (A_{glas}) according to the façade area ($A_{façade}$) of the windows used in the study at SBi and ISE

Institute	Small		Medium		Large	
	$A_{glas}/A_{façade}$ (%)	ω_s	$A_{glas}/A_{façade}$ (%)	ω_s	$A_{glas}/A_{façade}$ (%)	ω_s
SBi	≈25	1.12	≈44	2.00	≈85	3.89
ISE	≈21	0.96	≈45	2.06	≈89	4.21

The solid angle subtended by the source (ω_s) is the apparent size of the visible area of sky at the subject's eyes 1.5 m from the window.

Table 2
Optical properties of the sun shading systems used in the experimental set-up

No.	System, test location	Type	Colour and reflectance	Transmittance
1	Venetian Blinds ISE, SBi	80 mm, convex	White (RAL 9016, ρ_{vis} = 84%)	Tilt dependent
2	Venetian Blinds ISE, SBi	80 mm, concave	Top side mirror-finished (Miro 4, ρ_{vis} = 95%), lower side grey (RAL 7030)	Tilt dependent
3	Vertical Lamellas ISE	Transparent foil	n.a.	2%

It is expected that a fourth system (screen roller blinds with approx. 10% transmission) will be tested, but it is not included in this study.

Table 3
For the solar shading systems included and the three different window configurations tested, means, minimum, maximum and standard deviation of window luminances were measured with the CCD camera and averaged across all seating positions, view directions, times of day, weather types, and measurement days (Note that evaluation of the specular Venetian blinds at SBi are not included)

System	Window size	Number of tests	Mean (cd/m^2)	Minimum (cd/m^2)	Maximum (cd/m^2)	S.D. (cd/m^2)
White Venetian blinds	Small	85	3784	434	7412	1679
White Venetian blinds	Medium	86	3873	343	7269	1590
White Venetian blinds	Large	86	3596	342	6320	1546
Specular Venetian blinds	Small	19	5249	2044	9131	2341
Specular Venetian blinds	Medium	18	4435	1583	7147	1520
Specular Venetian blinds	Large	19	3937	2415	6120	1138
Vertical foil system	Small	12	569	80	980	354
Vertical foil system	Medium	12	297	74	584	190
Vertical foil system	Large	12	336	88	488	137
Total		349				

Seven tests have been discarded, because of set-up errors.

and analysing the luminance data of the whole recorded scene.

A separate exterior meteorological station located on the roof at both sites recorded global total and diffuse illuminance (LMT BAP30, Hagner ELV641) and irradiance (Kipp & Zonen CM 11) measurements. In addition, the vertical illuminance on the façade was recorded.

3.3. Procedure

At the beginning of an experimental session the subjects (in the test room) were asked about their general impression and opinion of the room, the windows and occurring glare problems. During the session, the subjects performed different tasks, such as reading from a paper, working on a computer, etc. similar to a normal situation where they typically perceive discomfort glare and veiling reflections. The task presentation order was fixed and data on users performance (speed and errors) were recorded. The main purpose of these work tasks was that all subjects performed the same office task during the tests before answering the questionnaire. Results of the performance measures are not included in this study. Osterhaus and Bailey [8] stated that no data is available on perceived comfort or discomfort in relation to comfort and task performance under conditions in which the glare source borders or surrounds a work task. Until that time, almost all previous studies evaluated discomfort glare by directly viewing the glare source rather than focusing on a work task.

The order of presentation of the three window sizes and two viewing directions (subjects were seated parallel with the window or diagonally towards the window) was carefully controlled to make sure that no single order would prevail over another. To reduce the number of subjects required, the principle of Latin Squares was used. The different combinations of window size appeared once and only once in each row and column of the matrix. Additionally, the presentation order for the different window sizes was counter-balanced with the two viewing directions. The viewing direction was either parallel with the window (90°) or facing diagonally towards the window (45°). Due to the time frame of the project, it was not

Fig. 2. Interior view of the work place with CCD camera at eye position and interior illuminance sensors in the reference room (parallel view set up) at the Danish Building Research Institute SBi (left) and at Fraunhofer ISE (right).

possible to make a within-subject design for all combinations of window sizes, viewing directions, and shading devices. Therefore, the evaluation of the glare assessment was made as a between-subject study. Subjects were mostly selected among employees of SBi and ISE (10% of the ISE subjects were external students), all of them were naïve users, which usually work in another area field (e.g. administrative assistants. . .).

One session lasted for about 1 h and 45 min, e.g. 10.00–11.45 and 12.15–14.00, given that 12.00 is the hour when the sun is perpendicular to the façade at SBi. Since the test facility at ISE can be fully rotated, starting times were not fixed. The test starting time at ISE was determined by the occurrence of similar sun heights as for the respective testing at SBi. During the session, only the window size was changed, which meant that the subject evaluated three different window sizes, each lasting about 30 min. During the change of window size, the subjects left the room for a 5-min break.

When the subjects entered the test room, the Venetian blinds were in a fixed position with maximum daylight coming into the room, maintaining some view to the outside, but allowing no direct sunlight to penetrate the solar shading device (''cut-off'' position). The foil system was completely closed. For a venetian blind the initial setting of the tilt angle of the blinds was the cut-off angle with a 5°–10° offset to ensure that no sunlight penetration occurred during the test. The subjects were not allowed to change the blind angle or position during most of the test.

Individual glare perception could differ from season to season, since subjects might have a higher acceptance of the presence of sunlight in the winter than in the summer [15]. In the experiment, no real distinctions between seasons were evaluated, but time-of-day was handled by having subjects assess the interior lighting conditions in the morning and afternoon sessions. The assessment of glare and the impact of different weather conditions (overcast, intermediate and clear sky) was out of the scope of this study. All tests within this study had been carried out under stable clear sky condition in order to prevent significant changes of the lighting situation.

No artificial lighting was added during the test, even if artificial lighting would ensure that the subjects did not have any problems with performing the tasks. In the studies conducted by Velds [16], the impact of artificial lighting contribution was found to be negligible. In the questionnaire, the subjects were asked whether they wanted some additional lighting, either through general lighting or through a moveable desk lamp.

3.4. Questionnaire on lighting conditions

The questionnaire on the lighting conditions was divided into four main parts. The demographic questions (part 1) considered gender, age, left or right handed, the wearing of glasses or contact lenses, and sensitivity to bright light. Questions in part 2 were related to rating the lighting conditions when reading, typing and performing letter-search tasks. The subjects described the perception of the visual conditions by means of a line rating scales, e.g. if they experienced any disturbing glare from the window or the shading device (not at all-very much). Furthermore, they were asked to associate the magnitude of glare on a four-point scale with pre-defined glare criteria (imperceptible, noticeable, disturbing and intolerable) and whether they would rate the lighting condition comfortable or uncomfortable, if they had to perform their daily work at the test work place. Part 3 was subdivided into two parts. The first part concentrated on general lighting conditions within the room before the subjects could change the system according to their wishes, while the second part concentrated on why they had changed the initial set-up of the solar shading system. Part 4 focused on indoor climate conditions in the room.

4. Results

4.1. Demographic characteristics of subjects and test conditions

Subjects evaluating the three different solar shading systems were mostly recruited at SBi and ISE. A total ($n = 76$) of 48 men and 28 women participated (SBi 13 men and 9 women; ISE 35 men and 19 women) ranging in age from 20 to 59 (SBi: $M = 43.4$, S.D. = 7.3, $n = 22$; ISE: $M = 25.8$, S.D. = 3.1, $n = 54$). Within the group, 33 subjects used glasses and six subjects used contact lenses. Almost all the subjects ($n = 72$) where right-handed. For the white Venetian blind, 44 subjects evaluated the system for a view direction parallel with the window and 45° diagonal towards the window.

The tests were conducted from September 2003 until the end of December 2004. A descriptive statistic of the window luminance data for three solar shading systems is shown in Table 3.

4.2. Interior measurements – illuminance

To ensure that both the test room and the reference room had the same illuminance level during the tests, two illuminance sensors were installed in both rooms at the same location. Figs. 3 and 4 show a comparison between the desk illuminance sensors on the work plane for all performed tests.

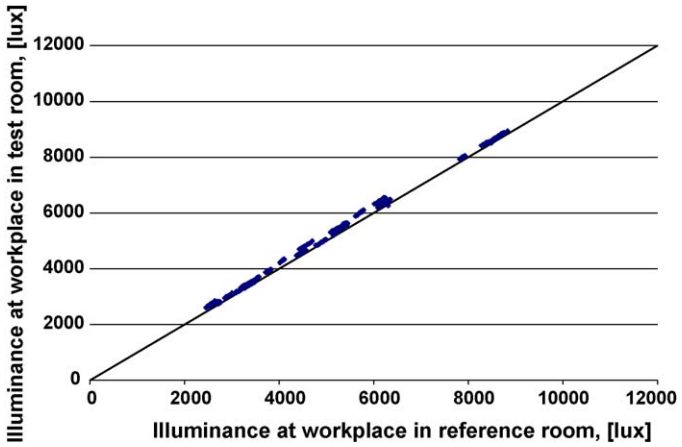

Fig. 3. SBi: comparison between desk illuminance in the two rooms. (*note*: only white Venetian blinds).

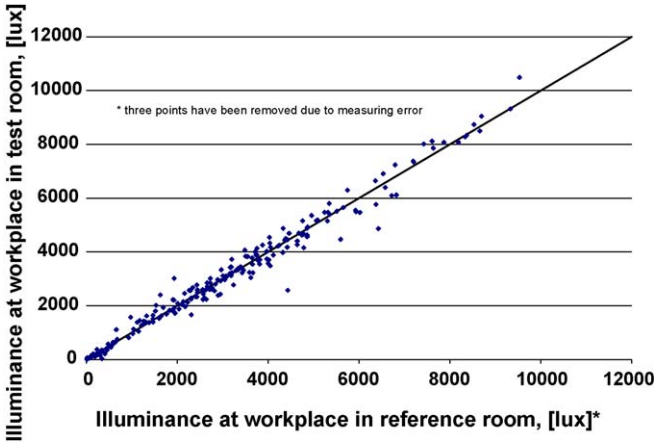

Fig. 4. ISE: comparison between desk illuminance in the two rooms. (*note*: all shading systems included).

The comparison showed that in most cases the illuminance level in the experimental rooms, at both locations, was very similar, and that there had been comparable interior lighting conditions at both locations. One explanation for the remaining differences could be that for Venetian blinds each slat might not be in exactly the same position in the two rooms. The desk sensor might differ slightly in position, since the subjects needed to have some space, while performing the work tasks. Light reflected from the subject's clothing might also have caused some of the differences. Nevertheless, the difference between the two rooms at each institute was regarded as not significant.

4.3. Interior measurements – luminance (CCD camera)

As a first step, the product-specific data format of the CCD camera-picture was converted into the RADIANCE [19] picture format in order to have a more commonly used data format. In addition to this, the RADIANCE picture format enables in principle the use of the new evaluation tool *evalglare* (see Section 4.4) for simulated scenes as well.

The reliability and data quality management of the acquired picture measurements was a very important item, since a huge amount of data was collected. At Fraunhofer ISE a luminance picture was acquired every 30 s, the reading of the illuminance sensors was stored every 10 s to ensure having enough data within the task periods of 4 min each. In total, more than 10,000 pictures and more than 30,000 illuminance values were acquired. Special routines were developed to filter out the related "right" picture and illuminance values for each task of the tests. For each selected picture a control image was created, containing all test and task information in order to get a comprehensible documentation (see Fig. 5). At SBi, a luminance picture was taken every 2 min (more than 3000 pictures), due to different type and set-up of the camera than Fraunhofer ISE. Interior illuminance data were stored every 30 s.

To check the integrity of the luminance picture, a comparison was made between the measured vertical illuminance above the camera with the integrated value of the related luminance picture. The correlation between measured and calculated vertical illuminance level on the eye is shown in the graphs of Fig. 6. The left graph of Fig. 6 shows the correlation between LMK Mobile and measurements (SBi, only white Venetian blinds), while the right graph of Fig. 6 shows the correlation between LMK 98 and measurements (ISE, complete data set). In both graphs the correlation is high, and for most cases the values are very similar. The remaining differences can be explained by the slightly different position of the lens and the illuminance sensor. In general these differences were regarded as minor important and therefore the pictures are trustable for further evaluations.

4.4. Glare source detection – evalglare

The technology of high dynamic picture mapping enabled a much more detailed evaluation of the visual environment than

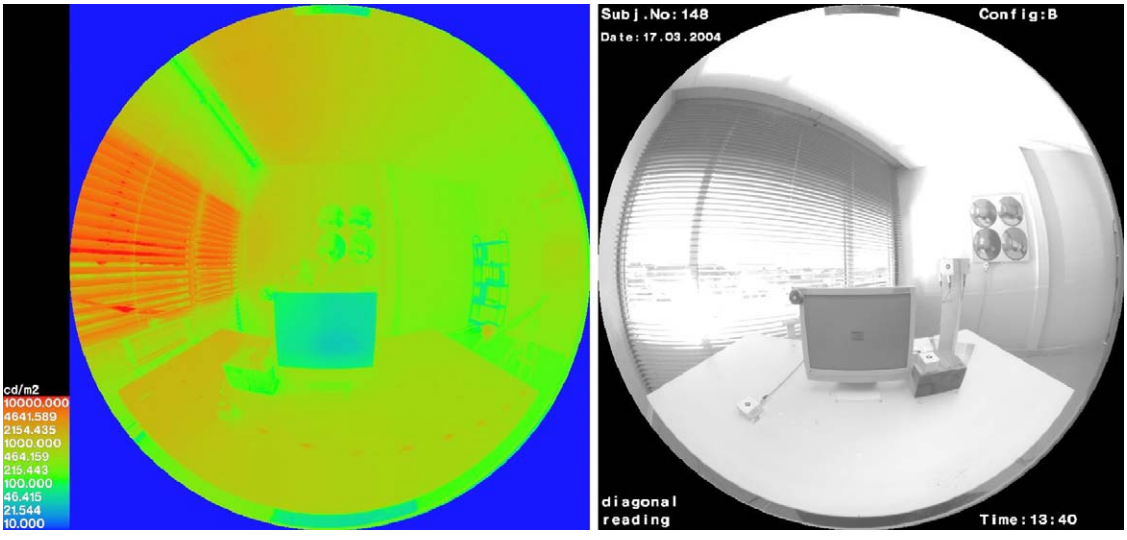

Fig. 5. Left: example of a luminance picture converted into RADIANCE picture format, displayed in a false colour scale. Right: example of a documentation control image with information about subject, date, time, façade configuration and type of task.

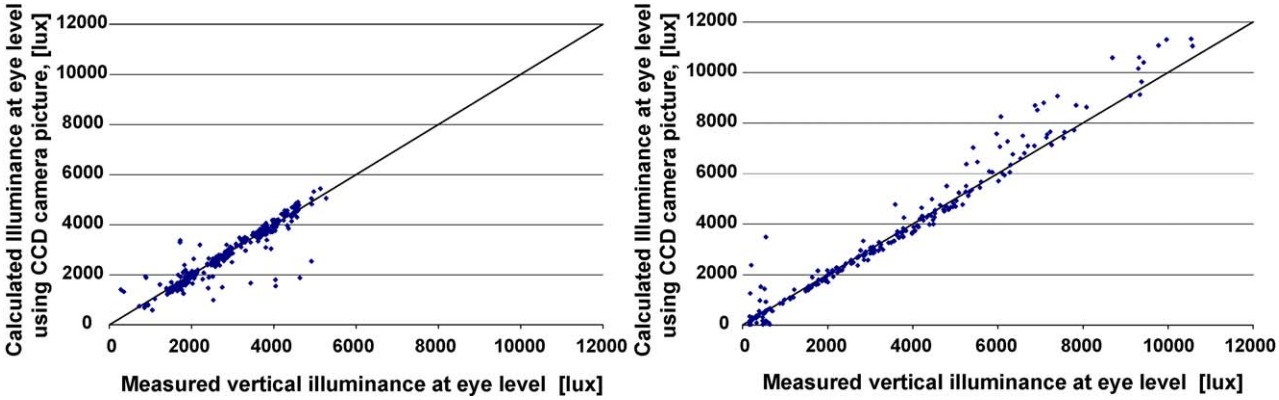

Fig. 6. Comparison between calculated and measured vertical eye illuminance, Left: SBi – only white Venetian blinds, Right: ISE – complete data set.

in the past – but it also led to new questions. One of those ''new questions'' was to determine the parts of the scene which should be treated as a ''glare source''. The human eye detects potential glare sources immediately, but in case of a picture evaluation, a detection algorithm is needed, which detects effectively and reliably all possible glare sources in very different lighting scenes.

Three principal methods were tested for the automatic detection of glare sources

1. Calculate the average luminance of the entire picture and count every section as a glare source that is x-times higher than the average luminance;
2. Take a fixed value and count every section as a glare source that is higher than the fixed value;
3. Calculate the average luminance of a given zone (task area) and count every section as a glare source that is *x*-times higher than the average luminance of this zone;

The first method was implemented in the RADIANCE *findglare* tool. For very bright scenes (e.g. white Venetian blinds in cut-off position on a fully exposed façade), only few parts or nothing could be detected, although the façade was obviously a glare source. Reducing the *x*-factor can increase the sensitivity to detect glare sources in a scene, but might lead to ''overdetecting'' potential glare sources in darker scenes.

The second method, which applied a fixed luminance value as threshold (e.g. 5000 cd/m^2) does not take into account eye adaptation. This method was therefore not considered to be a reliable method for lighting scenes with substantial luminance variations.

Finally we used the third method, by taking a ''task luminance'' as threshold for the glare source detection. In case of VDT tasks, a circular zone with an opening angle of about 0.53 sr was used as a target task-zone (see Fig. 7). The task-zone was chosen, so that it covers most parts of the computer screen and parts of the desk, while the window is not a part of the zone. Each pixel with a luminance value four times higher than the average task-zone luminance was treated as a glare source. This detection sensitivity factor can be changed. All three glare source detection algorithms were implemented into the new evaluation tool ''*evalglare*''. Evalglare also calculates the average luminance, the solid angle and the position within the picture for each glare source. With these values the validation with existing glare indices could be processed.

For each picture, all pixels exceeding the luminance threshold (four times higher than the average task-zone luminance value) are treated as glare source. These ''glare source pixels'' are combined to one large glare source, if the distance between the pixels is small. The search distance (search radius *r*) between each pixel can be changed by an option in the software-tool. There is no size limit of the glare source and no automatic subdivision of the glare source is implemented into the tool. Subdivision can lead to a different result but needs further investigation, which was beyond the scope of this study. Another issue was how to handle darker parts, such as window frames surrounded by the ''glare source pixels'' (see Fig. 8). Should they be taken into account as a part of the glare source or not? For that reason, a smoothing option was implemented. Applying the smoothing option to our

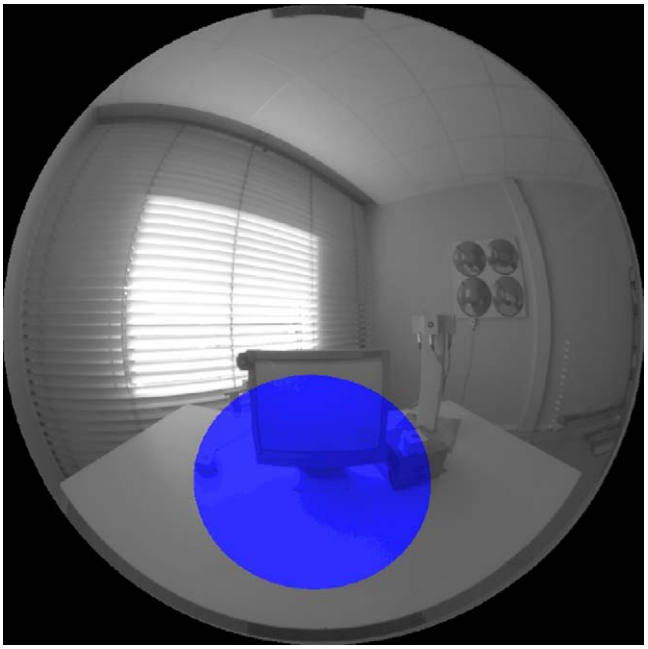

Fig. 7. Definition of the task-zone for the tests. Within the task-zone (coloured blue), the average luminance value was calculated (For interpretation of the references to colour in this figure legend, the reader is referred to the web version of the article.)

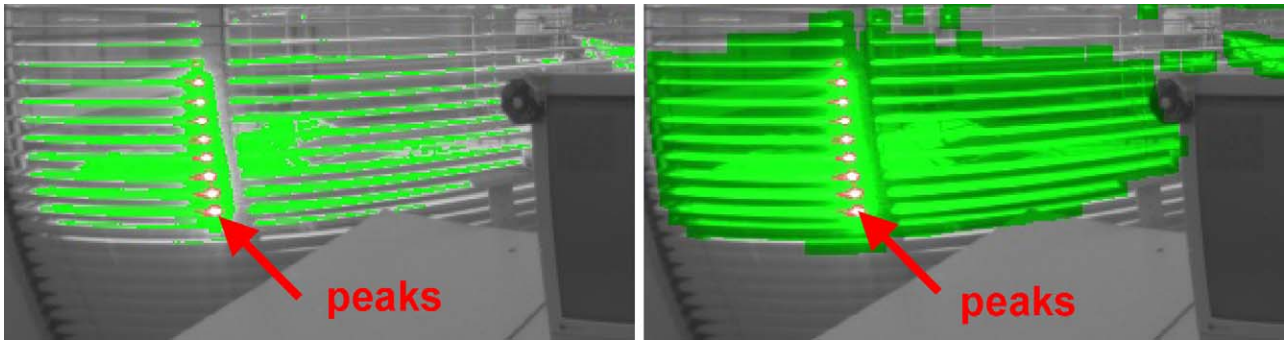

Fig. 8. Left: without the smoothing option, the darker (grey) parts (e.g. window frame) between the green-coloured ''glare source pixels'' were not taken into account as part of the glare source. Right: the smoothing option included the darker parts into one glare source, since these parts were surrounded by a glare source. In both pictures: high luminance peaks were extracted to a separate glare source (For interpretation of the references to colour in this figure legend, the reader is referred to the web version of the article.)

pictures had limited impact and raised additional questions (see Section 5.2.2 and Fig. 16).

Solar shading systems or innovative daylighting systems can reflect the image of the sun to be seen from the viewpoint. Reflected sunlight can often cause high localised luminance peaks, but adding those ''peaks'' into a large glare source might not increase the total luminance of the glare source significantly, due to size of the source. The *evalglare* tool has an option to extract these luminance peaks and treat them as separate glare sources. A simple threshold criterion was used to extract the peaks (Fig. 8). For the present data, a value of 50,000 cd/m^2 ended up with reasonable results, because in many pictures large areas showed luminances higher than 5000 cd/m^2. And since the peaks should have a significant higher value than the surrounding, 50,000 cd/m^2 was chosen as threshold. More complex extraction functions were tested, but showed no significant improvement.

A special feature of the *evalglare* tool is an optional provision for colouring detected glare sources (the rest of the picture is set automatically to grey). This option was very useful for verifying different potential glare sources (Fig. 9).

4.5. Calculation of the position index

The position index expresses the change in discomfort glare experienced relative to the angular displacement (azimuth and elevation) of the source from the observer's line of sight. The analytical description for the position index located above the line of vision is [18]

$$\ln P = [35.2 - 0.31889\tau - 1.22\mathrm{e}^{-2\tau/9}] \times 10^{-3}\sigma + [21 + 0.26667\tau - 0.002963\tau^2] \times 10^{-5}\sigma^2 \quad (6)$$

where τ is the angle from vertical of plane containing source and line of sight [°] σ is the angle between line of sight and line from observer to source [°].

In a study by Iwata and Tokura [17], the sensitivity to the glare caused by a source located below line of vision was found to be greater than the sensitivity to glare caused by a source above line of vision. In the discussion of results, Einhorn expressed an analytical equation for a source located below the line of vision of the results found in [17]

$$\begin{aligned} P &= 1 + 0.8 \times \frac{R}{D} \quad \{R < 0.6D\} \\ P &= 1 + 1.2 \times \frac{R}{D} \quad \{R \geq 0.6D\} \\ R &= \sqrt{H^2 + Y^2} \end{aligned} \quad (7)$$

where

D is the distance eye-to plane of source in view direction;

H is the vertical distance between source and view direction;

Y is the horizontal distance between source and view direction.

Fig. 10 shows the application of both equations on a fish eye view (180°). Both equations were implemented in the *evalglare* tool to calculate the position index.

4.6. Calculation of the façade luminance

To evaluate potential glare sources in an office space, the estimation of average façade or window luminance is an important measure. Within the experimental set-up, we experienced that an automatic calculation of the façade and window luminance is complicated because the position of the window and view direction changed and the picture has no geometric information about the scene. To handle this we extracted these data by using picture masking. The mask ''cuts out'' only the window and sets the remaining pixels to zero. Further processing extracts the luminance value of the ''non-zero'' pixels and calculates the average façade luminance (Fig. 11).

5. Correlation between user response and glare evaluation methods

5.1. Correlation towards existing methods

Most of the existing glare indices try to estimate possible glare sensation of a so-called ''standard observer''. Although this is not completely wrong, a word of warning is needed, since large variations of rating discomfort glare are normally found when comparing individual subjects. Also, Velds [16] stated

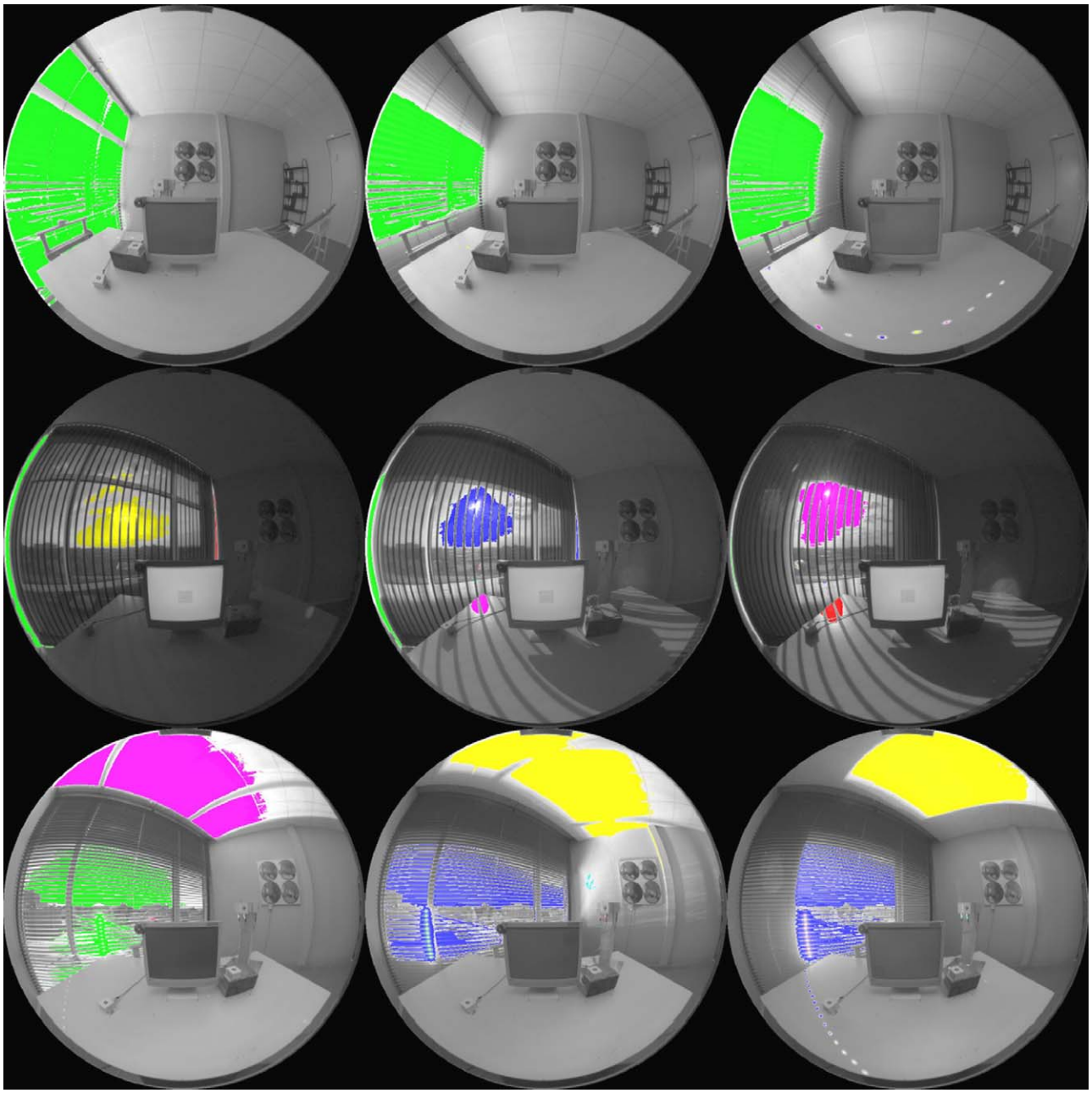

Fig. 9. A set of typical pictures of luminance pictures converted to the RADIANCE pic-format and evaluated by *evalglare* tool. First row: white Venetian blinds, second row: vertical foil system, third row: specular Venetian blinds. Each blind is shown for each window size. The specular Venetian blinds redirected light to the ceiling (more than 10,000 cd/m^2 in some cases). These areas were also detected as glare sources.

that the majority of existing glare equations were developed for the evaluation of discomfort glare from small artificial light sources and cannot be used for the assessment of discomfort glare from windows, because the source size mostly subtends a solid angle at the eye that exceeds 0.01 steradians. Another issue is that current glare indices cannot reliably predict the level of discomfort glare from daylighting in a working environment with normal work activities and complex non-uniform glare sources, such as a venetian blind system.

In Fig. 12 the DGI and the CGI for all 349 cases are drawn versus the glare rating. It can be clearly seen that the individual difference in perceiving glare led to a wide spread of the data, so that in this comparison no correlation could be found. The same occurred for all other existing glare equations.

An approach to overcome the difficulties of how to treat individual differences in perceived glare was to use the probability if a person was disturbed instead by the glare magnitude. For that reason, the glare scale was reduced to two categories. A category ‘‘disturbed’’ was used if the subject rated the glare source to be ‘‘disturbing’’ or ‘‘intolerable’’. The probability was established by grouping equal sample sizes (e.g. 29) of the total of 349 different cases and evaluating the percentage of disturbed subjects in each of these ‘‘classes’’. A sample size of 29 therefore led to 12 classes. The classes were

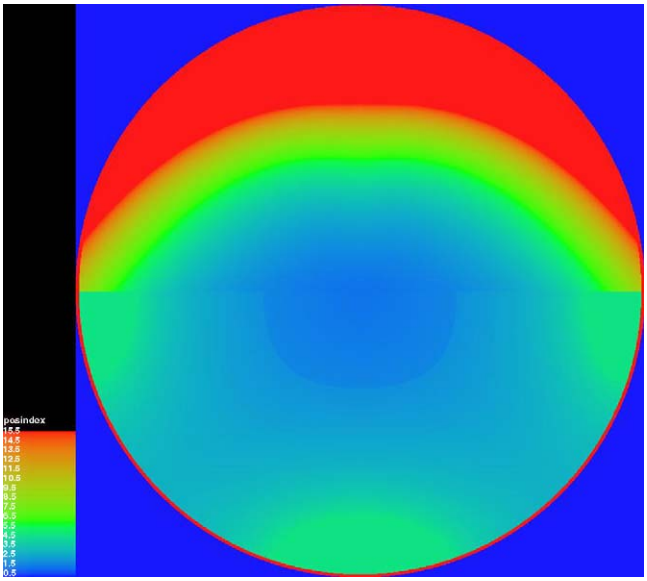

Fig. 10. The position index expresses the change in discomfort glare experienced relative to the angular displacement (azimuth and elevation) of the source from the observer's line of sight. The figure shows (fish-eye view) the analytical expressions for the position index located above [18] and below [17] the line of vision for a horizontal view.

established by grouping the different cases by the glare measure (e.g. DGI, CGI, window luminance) first in order to have similar values in each class. This means that the different cases were grouped differently for different glare measures. In each class, the glare measure (e.g. DGI, CGI, window luminance) was averaged to one value. In the following graphs the relationship between the "disturbing" probability and three existing measures is shown. In many regulations especially in Europe, the window luminance is used as a measure for glare and is restricted to a certain value. But it can be clearly seen in Fig. 13 that there exist no correlation between the window luminance as glare measure and the user response. The main reason for this is that the solid angle of the window is not taken into account.

Better correlations could be found for the DGI and CGI. But the spread of these existing measures was still high, taking into account that the classification process averaged the results and rises in principle the correlation.

5.2. *Development of a new glare equation – daylight glare probability*

As discussed in the previous paragraph our new approach uses the probability that a person is disturbed instead of the glare magnitude as a glare measure. This new probability function is called "daylight glare probability, DGP".

As a first approximation, we used the vertical illuminance at the position of the subject's eyes, facing the same view direction, as a basis for the probability. Two different forms of the equation are tested: a linear (8) and a logarithmic (8a) approach.

$$\mathrm{DGP} = c_1 E_\mathrm{v} + c_2 \tag{8}$$

$$\mathrm{DGP} = c_1 \log(E_\mathrm{v}) + c_2 \tag{8a}$$

Velds [16] stated that using two vertical illuminance sensors facing the window and the wall, showed high correlation with subjective glare ratings in situations without a daylighting system (blinds), but also that this is not the only parameter in glare assessment. Interesting results of the experiments show that the logarithmic approach has lower correlation than the linear approach, although we expected, due to the law of Weber-Fechner, the results to be reverse (see Fig. 14).

Fig. 11. Left: original luminance picture, Right: the window was masked and the remaining pixels were set to zero. The masking process also took into account that the VDT screen and the work plane shaded parts of the window.

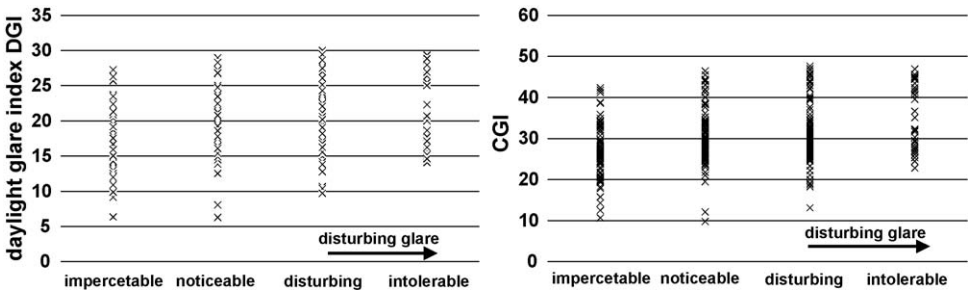

Fig. 12. Calculation of existing glare ratings showed a large variation of rating discomfort glare (left DGI, right CGI).

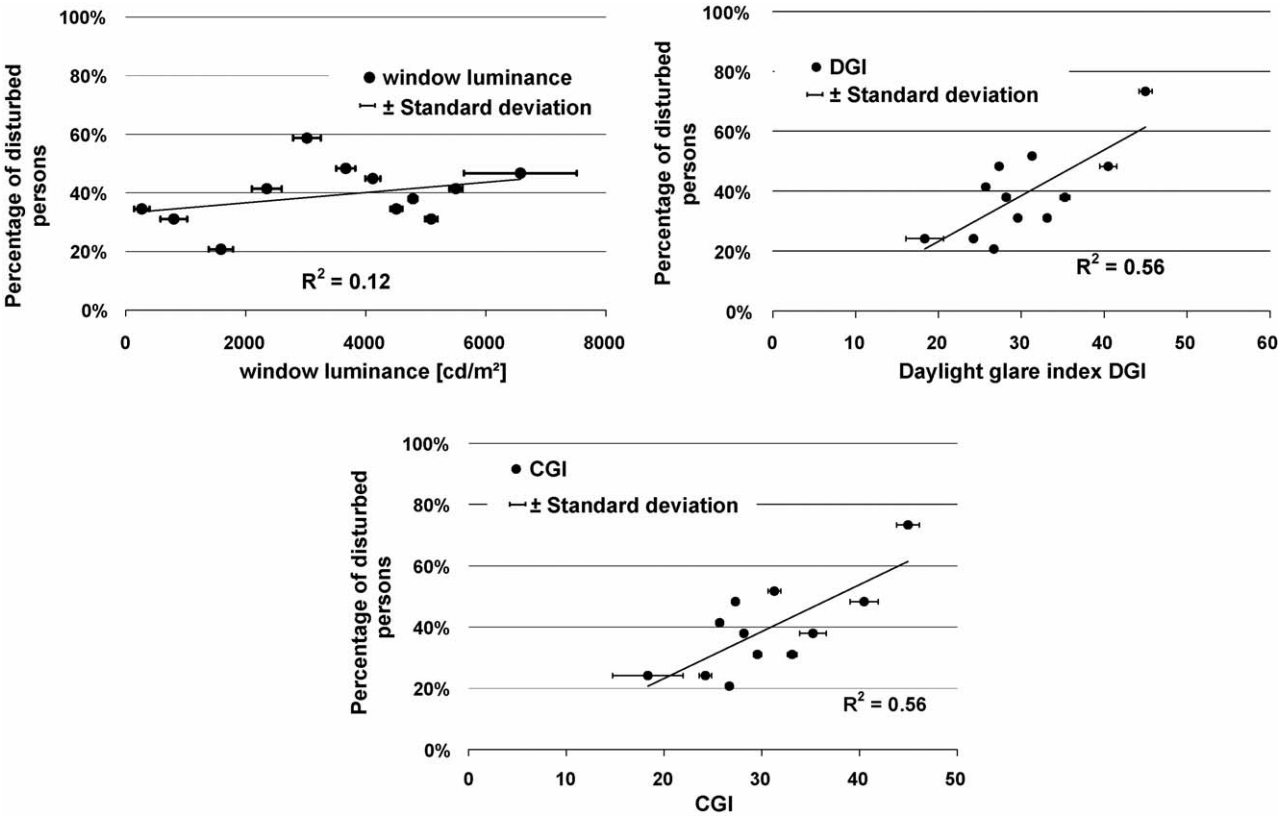

Fig. 13. The relationship between the disturbing probability and the three glare measures DGI, CGI, and window luminance.

The correlation between the linear function of vertical eye illuminance and the probability of disturbed persons was stronger than all other tested functions. The problem with this form of the function was that it does not take into account individual glare sources, but only the total amount of light at eye-level.

Detailed investigations showed that the correlation between user reaction and DGP could be improved by taking into account the individual glare sources of each situation. The basic idea to improve the new DGP formula was a combination of using the vertical eye illuminance as glare measure, using the central sum of the glare source term of CIE glare index and using an empirical fit of some parameters. Furthermore, the use of L_b as measure for the adaptation level is not suitable, since the large glare sources themselves have impact on the adaptation level. Therefore, the authors suggest to use the vertical eye illuminance E_v as measure for the adaptation level. This hypothesis was also supported by achieving somewhat higher correlations for E_v than using L_b for the adaptation term in the equation. The structure of the equation is then

$$\mathrm{DGP} = c_1 E_v + c_2 \log\left(1 + \sum_i \frac{L_{s,i}^2 \omega_{s,i}}{E_v^{c_4} P_i^2}\right) + c_3 \tag{9}$$

For optimizing the parameters $c_1, \ldots, c_4$ all detected glare sources for each of the 349 cases were written into a file and

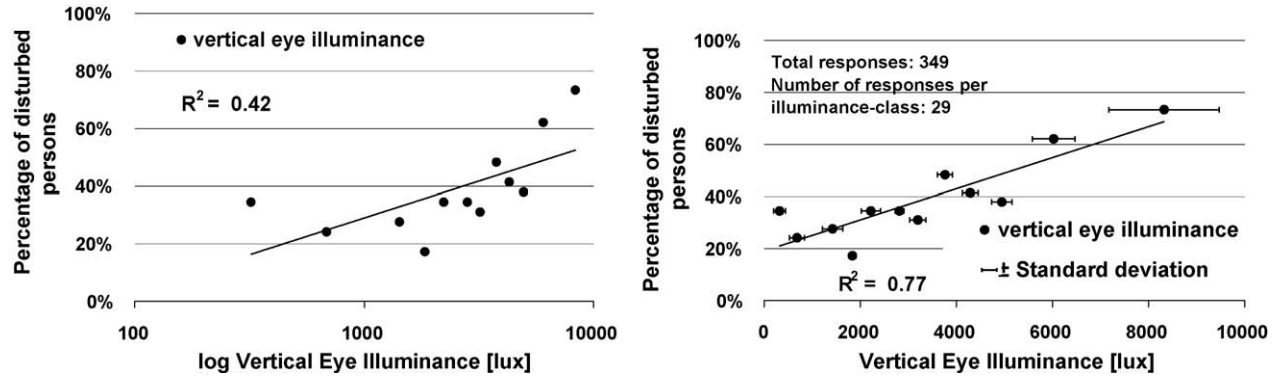

Fig. 14. The daylight glare probability function, using the vertical illuminance at the position of the subject's eyes (E_V) as a basis. Left figure show the logarithmic function of E_V, and right figure show the linear function of E_V. The functions do not take into account individual glare sources. The valid range of the linear function is expected to be within 1000 lux to almost 10,000 lux.

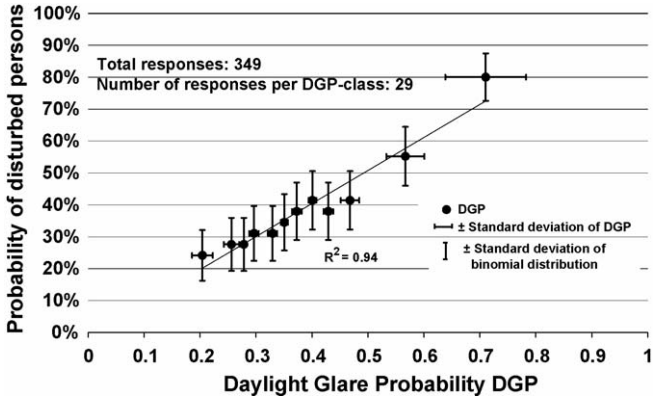

Fig. 15. Correlation between the new DGP formula and the probability of disturbed persons in the tests. A DGP value higher than 0.2 approximately corresponds to a vertical eye illuminance higher than 1000 lux. Subjective glare rating included in the graph consisted mostly of subjects evaluating the white Venetian blinds (not causing severe glare sensation). As the white Venetian blinds did not cause a severe glare sensation, the majority of established classes were in the lower part of the function.

merged with the subject's glare rating. Using a random optimisation algorithm, thousands of different parameter settings were tested. Highest correlation with subjective glare rating were found with the following parameter settings (see also Fig. 15)

$$\mathrm{DGP} = 5.87 \times 10^{-5} E_\mathrm{v} + 9.18 \times 10^{-2} \log\left(1 + \sum_i \frac{L_{\mathrm{s},i}^2 \omega_{\mathrm{s},i}}{E_\mathrm{v}^{1.87} P_i^2}\right) + 0.16 \quad (10)$$

where E_v is the vertical eye illuminance [lux]; L_s the luminance of source [cd/m^2]; ω_s the solid angle of source; P is the position index, based on Fig. 10.

The validity of the equation is within the range of the tests, which means a DGP value between 0.2 and 0.8. In the authors point of view, calculated values higher than 0.8 could be trusted to some extend, since the comparison of 10 cases with the highest DGP-values also gave reasonable results (average DGP was 80% by having 100% disturbed persons). DGP values lower than 0.2 should not be used unless additional experiments could confirm the validity of the equation in that region.

5.2.1. Significance of the DGP equation improvement

Adding parameters to an equation, which are fitted to the data usually lead to higher correlations – but this does not automatically mean, that this optimised equation describes the behaviour better. The authors do not believe there are any well defined statistical tests to unambiguously determine statistical significance for this non-linear and group changing problem. However, the standard F-test for multi-linear regression should provide a reasonable check of plausibility. Failure to pass the F-test is a fairly clear indication that the added parameters are not providing significant improvement – but passing the test is only a good indicator that there could be an improvement. In our case, we used the vertical eye illuminance Eq. (8) as basis for the test, since this is the best two parameter fit to the experimental data, better than CGI or DGI, which are also both two parameter fits. The original data set consist of 349 data points, which have been reduced due to the necessary grouping to 12 points.

The F-test value is calculated with following formula

$$F = \frac{(r^2_{\mathrm{DGP}(10)} - r^2_{\mathrm{DGP}(8)})\mathrm{DF}(\mathrm{DGP}(10))}{j(1 - r^2_{\mathrm{DGP}(10)})}. \quad (11)$$

with

$r^2_{\mathrm{DGP}(10)}$ is the squared correlation of Eq. (10), equals 0.94 here;

$r^2_{\mathrm{DGP}(8)}$ the squared correlation of Eq. (8), equals 0.77 here;

DF(DGP(10)) the degree of freedom of fit for Eq. (10), equals 8 here;

j is the number of added parameters to the fit, equals 2 here.

For this study the F-test value is 11.5. The significance value of this is given by the F-distribution-function and is calculated then to 0.0045, which is factor of 10 less than the limit of 0.05. Therefore, the Eq. (10) passed the F-test.

Nevertheless, the authors recommend confirming this new DGP Eq. (10) by other user assessments.

5.2.2. Influence of detection parameters

The influence of changing the primary detection parameter, the search radius r, within the *evalglare* tool, is illustrated in Fig. 16. A search radius within the range of 0–0.8 sr showed no significant change of the correlation and the influence of the search radius is limited. Search radiuses higher than 0.8 sr combined all detected glare pixels to few or one single glare source, which is different to the idea to weight the glare sources and relate the magnitude and individual position within the field of view. Search radiuses less than 0.01 led to treat every glare source pixel as separate glare source, due to the resolution of the camera.

Using the smoothing option does not improve the results, but the statistical spread slightly increase if the search radius is changed (see Fig. 16). The results could be improved, if the inclusion distance of the smoothing function is independent on the search radius, which is actually not the case. This needs further investigation.

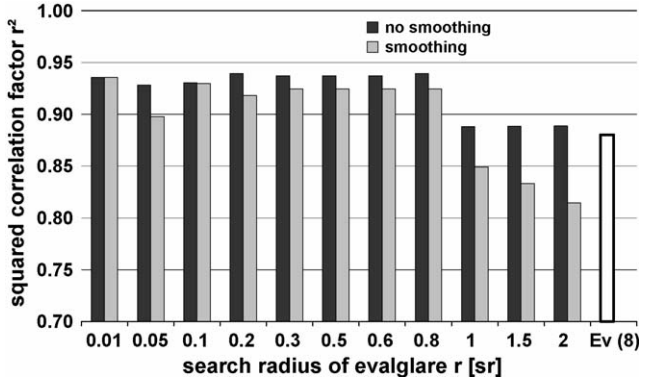

Fig. 16. Influence of the search radius on the squared correlation of the DGP function. The black bar is the used search radius of 0.2 sr. The white bar on the right hand side shows for comparison reasons the squared correlation factor for the vertical illuminance only (Eq. (8)).

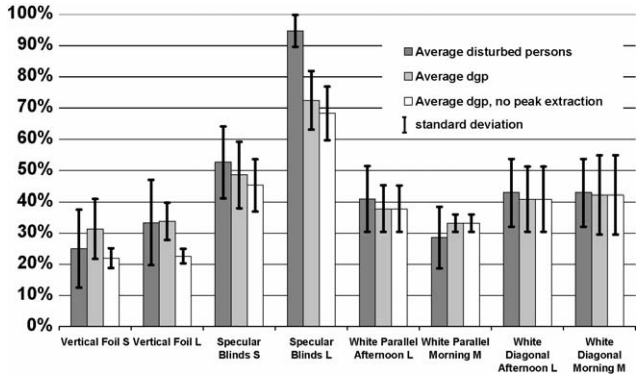

Fig. 17. Comparison of the DGP with the probability of disturbed subjects, grouped by the solar shading systems and window size (S: small, M: medium, L: large), and with two detection parameter sets – with and without peak extraction. The DGP showed reasonable correlation, even with 'extreme' conditions like a fully glazed façade with specular blinds.

Another question was how precise the new DGP could reproduce the assessment of the users, if the grouping method was changed. One possibility was to make groups according to different solar shading systems and window sizes (see Fig. 17). This changed the different group sizes and resulted in higher standard deviation of the DGP, since individual glare evaluation was carried out under different interior conditions within each group. Yet, calculation of DGP still follows the real number of disturbed persons reasonably well. Fig. 17 also showed that using the peak extraction parameter improved the results, especially for a solar shading system producing very high luminance peaks as the specular blinds do.

6. Discussion and conclusion

The use of CCD camera-based luminance mapping technology to measure luminances within the field of view, provides a great potential for improved understandings between measurements and user response. In our view, it is essential to use the CCD technology to assess, e.g. limits of acceptance for luminances and their ratios within the field of view for different sky and solar shading control conditions. The CCD technology also simplifies what was earlier a tedious measurement technique, since luminance measurements at specific 'spots' using a point-by-point measuring technique require an enormous amount of time, can only be achieved in a grid or was almost impossible to carry out. Although the CCD camera enables us to study the visual environment in detail as well as some of its parameters affecting the user, it also needs a lot of effort to extract the 'correct' values for the evaluations and to ensure high data quality.

The new evaluation tool *evalglare* can manage these evaluations and detect, effectively, all possible glare sources within very different lighting scenes. The tool also enables assessments of possible glare problems with simulated RADIANCE pictures, and could therefore be used at an early stage in the design of a building.

Using the tool for this study, we calculated several currently available glare prediction models and found that these indices showed a weak correlation with how subjects reported discomfort glare in an experimental set-up with three different façade layouts, two different view directions and three different solar shading systems. Due to the above uncertainties with the currently available glare prediction models, we propose a new glare equation, called "daylight glare probability (DGP)", where we use a combination of an existing discomfort glare algorithm and an empirical approach. The evaluation of the results from the experiments shows good correlation between the DGP and the user's response. The authors rate the new DPG as a reliable tool in many office situations, since the model is based on 349 different cases with more than 75 different subjects in two countries. Nevertheless, the new equation should be confirmed by additional assessments. The probability model should also be tested in conjunction with other solar shading systems. However, additional parameters, e.g. quality of view to the outside, are desirable to ensure the validity of the equation in most common office buildings.

In the experiments we recorded a rich data set containing illuminance measurements (inside, outside), more than 13,000 luminance pictures, and answers to a very detailed questionnaire. The data set provides ample opportunity for further analysis of, e.g. contrast ratios or user reactions to windows and shading devices.

Acknowledgements

The EU Commission supported the preparation of this paper, as part of the EU project "Energy and Comfort Control for Building management systems" (ECCO-Build, Contract No.: ENK6-CT-2002-00656). Authors acknowledge the ECCO-Build partners Fraunhofer Institute for Solar Energy Systems (D), Danish Building Research Institute (DK), Ingélux S.A.R.L. (F), Swiss Federal Institute of Technology in Lausanne (CH), Hüppelux (ex-Hüppe Form) (D), TechnoTeam (D), Bug-Alu Technic AG (AU), Servodan S/A (DK) for their contribution to this paper. We would like to thank especially the scientific project partners Marc Fontoynont, Tilmann E. Kuhn, David Lindelöf, Christophe Marty and Nicolas Morel for their valuable advice and the productive discussions. We thank Christian Reetz, Florian Pfeifer, Ulla Knapp, Thomas Haussmann, Alexander Adlhoch at Fraunhofer ISE and Steen Traberg-Borup, Boye Hørbye, Gunnar Holm, Kjeld Johnsen, Peter Mossing, Winnie Larsen at SBI for their contributions to this project. We will also thank Staffan Hygge (HIG), Werner Osterhaus (Victoria University of Wellington), Udo Krueger (TechnoTeam) and Bob Clear (Lawrence Berkeley National Laboratory), for their valuable advice and generous support.

References

[1] K. Rangi, W. Osterhaus, Windowless environments: are they affecting our health? in: Proceedings of LIGHTING '99 – Then, Now & Beyond, 44th Annual Convention of the Illuminating Engineering Society of Australia and New Zealand (IESANZ), Adelaide, Australia, October 18–19, 1999, pp. 4:9:1–4:9:13.

[2] J. Christoffersen, J. Wienold, Monitoring Procedure for assessment of user reaction to glare, Report ECCO-DBUR-0303-01 (Internal, but available,

when project completed), Energy and Comfort Control for Building management systems (ECCO-Build), EU Commission (Contract No: ENK6-CT-2002-00656), 70 pp., 2004.
[3] R.G. Hopkinson, P. Petherbridge, J. Longmore, Daylighting, Heinemann, London (UK), 1966, pp. 606.
[4] CIE, Discomfort Glare in the Interior Working Environment, Publication CIE No. 55 (TC-3.4), Commission Internationale de l'Éclairage (CIE), Vienna, Austria, 43 pp., 1983.
[5] P. Petherbridge, R.G. Hopkinson, Discomfort Glare and the Lighting of Buildings, Transaction of Illuminating Engineering Society 15 (39) (1950), London, UK.
[6] R.G. Hopkinson, Glare from daylighting in buildings, Applied Ergonomics 3 (4) (1972).
[7] W.K.E. Osterhaus, Discomfort glare from large area glare sources at computer workstations, in: Proceedings of the 1996 International Daylight Workshop: Building with Daylight: Energy Efficient Design, University of Western Australia, Perth, Australia, (1996), pp. 103–110.
[8] W.K.E. Osterhaus, I.L. Bailey, Large Area Glare Sources and their Effect on Discomfort and Visual Performance at Computer Workstations, Report LBL-35037 UC-350, Lawrence Berkeley National Laboratory, Berkeley, California, USA, 5 pp., 1992.
[9] J. Chauvel, B. Collins, R. Dogniaux, J. Longmore, Glare from windows: current view of the problem, Lighting Research and Technology 14 (1) (1982) 31–46.
[10] T. Iwata, K. Kimura, M. Shukuya, K. Takano, Discomfort caused by wide-source glare, Energy and Buildings 15–16 (1990/91) 391–398.
[11] M. Boubekri, L.L. Boyer, Effect of window size and sunlight presence on glare, Lighting Research and Technology 24 (2) (1992) 69–74.
[12] H.D. Einhorn, A new method for the assessment of discomfort glare, Lighting Research and Technology 1 (4) (1969) 235–247.
[13] H.D. Einhorn, Discomfort glare: a formula to bridge differences, Lighting Research and Technology 11 (2) (1979) 90–94.
[14] CIE, Discomfort Glare in the Interior Lighting, Commission Internationale de l'Éclairage (CIE), Technical committee TC-3.13, Division 4, Interior Environment and Lighting Design, Vienna Austria, 1992.
[15] J. Christoffersen, E. Petersen, K. Johnsen, O, Valbjørn, S. Hygge, Vinduer og dagslys – en feltundersøgelse i kontorbygninger (Windows and Daylight – a Post-occupancy Evaluation of Offices), SBI-rapport 318, Statens Byggeforskningsinstitut, Hørsholm (Denmark), 71 pp. (in Danish), 1999. (English: Windows and Daylight – A Post-Occupancy Evaluation of Danish Offices, J. Christoffersen, K. Johnsen, E. Petersen, O. Valbjørn, S. Hygge, Lighting 2000 – ILE/CIBSE Conference, NewYork, UK, July 9–11, 2000).
[16] M. Velds, Assessment of Lighting Quality in Office Rooms with Daylighting Systems, PhD thesis, Technical University of Delft, Delft, The Netherlands, 209 pp., 2000.
[17] T. Iwata, M. Tokura, Position Index for a glare source located below the line of vision, Lighting Research and Technology 29 (3) (1997) 172–178.
[18] IES Lighting Handbook, Reference Volume, Illuminating Engineering Society of North America, 1984, pp. 9–46, 9–49.
[19] W. Gregory, A.S. Robert, Rendering with Radiance, W.L. Greg, L. Gregory (Eds.), Morgan Kaufmann Publishers, 664 pp., 1998, ISBN 1558604995.